Article

Calibration and application of a sediment accumulation rate model – a case study

Rakesh K Gelda[1]*, Steven W. Effler[1], David A. Matthews[1], Emmet M. Owens[1], Craig A Hurteau[1], Steven C. Chapra[2], Martin T. Auer[3], Rasika K. Gawde[3], and H. Chandler Rowell[4]

[1] *Upstate Freshwater Institute, PO Box 506, Syracuse, NY 13214*
[2] *Department of Civil and Environmental Engineering, Tufts University, Boston, MA 02155*
[3] *Department of Civil and Environmental Engineering, Michigan Technological University, Houghton, MI 49931*
[4] *New York State Department of Environmental Conservation, Lake Service Section, Albany, NY 12233-3502*
** Corresponding author email: rkgelda@upstatefreshwater.org*

Received 17 October 2011; accepted 1 January 2012; published 28 February 2012

Abstract

A mechanistic mass balance model for sediment accumulation rate (SAR) that accommodates the dry density and burial velocity of solids and the depth dependency of porosity was tested and applied to Onondaga Lake, New York, for a 130-year period. The modeling for this case study is supported by a rich history of multiple anthropogenic drivers and coupled date horizons from the paleolimnological record, characterization of physical attributes of the sediments, and long-term monitoring of the water column and lake inputs. The consistency of predictions of SAR and measurements of downward flux of suspended particulate material (DF_{SPM}) from a long-term sediment trap program was also evaluated. The model was demonstrated to perform well in simulating the lake's history of SAR, which was supported by 10 different depth–date horizons. This history for 100 years was regulated by the production of soda-ash at an adjoining industry, which enhanced autochthonous formation and deposition of calcium carbonate ($CaCO_3$), proportional to the level of production of this chemical. The SAR was extraordinarily high (~5 kg m^{-2} yr^{-1}) during the 40 years of peak soda-ash production. An abrupt, more than 2-fold decrease in SAR occurred when the industry closed. The contemporary SAR remains relatively high as a result of multiple drivers but is serving to enhance burial of contaminants, including mercury, as part of an ongoing rehabilitation program. A high level of consistency (within 30%) between the contemporary SAR and an annual estimate of DF_{SPM} was documented. The utility of the model was demonstrated through applications that depict the amount of deposits contributed by the industry, the effect of compaction on burial velocity, the dilution effect of the high SAR values on the paleolimnological record, and the resolution of sediment diagenesis kinetics.

Key words: burial velocity, calcium carbonate, paleolimnology, mass balance modeling, sediment accumulation rate, sediment compaction

Introduction

Incorporation of depositing particulates into sediments is an important pathway for many constituents in aquatic ecosystems (Bloesch 2004) and in the cycling of those materials that are subject to diagenesis (Matisoff and Holdren 1993, Dittrich et al. 2009). The sediment accumulation rate (SAR), driven by deposition from the water column, is a fundamental metric for lake ecosystems and associated anthropogenic effects (Rippey et al. 2008, Rose et al. 2011) that structures the paleolimnological record with respect to the sediment depth and solid phase concentrations (dilution effect) of constituent horizons. Rose et al. (2011) reported increases in SAR in many

European lakes during the second half of the 20th century from an array of anthropogenic drivers, such as increased inputs of (1) autochthonously produced organic material, (2) allochthonous minerals, or (3) autochthonously precipitated minerals (Stabel 1986).

Accurate representation of SAR is an important feature of (1) paleolimnological analyses, (2) mechanistic ecosystem sediment models designed to simulate both deposition and diagenesis-based mobilization of various constituents (Dittrich et al. 2009; SC Chapra, MT Auer, RK Gawde, RK Gelda 2011, unpubl. data), and (3) rehabilitation programs that depend on burial of constituents (USEPA 2005). SAR can be determined through profiles of certain radioisotopes (Rose et al. 2011) or by identifying sediment depth horizons of various characteristics that can be coupled to historic events. Mechanistic ecosystem models are invaluable in testing the understanding of regulatory process and in providing a quantitative framework to support analyses and projections for changes in drivers of both research and management interest (Chapra 1997). SAR models are particularly valuable for those lakes that have experienced changes in deposition rates in response to anthropogenic drivers, and where SAR magnitude is important to management deliberations concerned with diagenesis-based feedback (Dittrich et al. 2009) and contaminant burial (USEPA 2005).

Properly designed sediment traps (Bloesch and Burns 1980, Blomqvist and Hakanson 1981, Bloesch 1996) are used to quantify deposition (downward flux) at shorter time scales than can be resolved through the sedimentary record. The consistency between trap measurements and SARs determined through analyses of sediment cores provides context for the interpretations of respective observations and their effective integration into related modeling and sediment-based rehabilitation programs.

This paper describes the development, testing, and application of a mechanistic mass balance model for SAR for a polluted lake for a 130-year period. The mass balance constructs of the model are broadly applicable and particularly valuable where changes in SAR have been experienced in response to anthropogenic drivers. The case study for this lake tested the hypotheses that (1) waste inputs from a local industry were primarily responsible for the increase in SAR, and (2) the increases were linearly related to chemical production by that industry. Moreover, the consistency between deposition fluxes determined from a long-term sediment trap program (Hurteau et al. 2010) and SAR values based on modeling of the paleolimnological record was evaluated. The calibrated SAR model was applied to provide insights on sedimentary processes, including the interplay between SAR and horizon depth features of the paleolimnological record, the effects of compaction on burial rate, and diagenesis kinetics. This is a particularly valuable case study of SAR modeling because (1) it represents an extreme, or end-member, case with respect to magnitude and robust dynamics, in response to an anthropogenic driver; (2) cause and effect is clearly resolved; (3) model testing is supported by a unusually rich paleolimnological record; (4) the long-term sediment trap record of deposition rates provides a consistency check; and (5) it supports multiple initiatives for rehabilitation of this lake.

Methods

System description

Onondaga Lake is an alkaline, calcium (Ca^{2+})-rich system located 43º06′54″N, 76º14′34″W in metropolitan Syracuse, New York, USA. (Fig. 1). The lake has a surface area of 12.0 km^2, a volume of 131 × 10^6 m^3, and a maximum depth of about 20 m. This lake is dimictic with strong stratification during the summer months (O'Donnell et al. 2010). The lake responds rapidly to changes in external loading because of its rapid flushing rate (~4 times per year; Doerr et al. 1994). Onondaga Lake was oligomesotrophic before European settlement in the late 1700s (Rowell 1996). Sediment core analyses indicate the pelagic sediments were enriched with calcium carbonate ($CaCO_3$) before that era (Rowell 1996, Rowell and Effler 1996). The depositional portion of the lake basin corresponds to depths >8 m, which represents approximately 65% of the total sediment area (Auer et al. 1996).

As the area developed, inputs of industrial and domestic wastes to the lake increased, which led to severe degradation of water quality (Effler 1996). Our review of this history for this study is selective (Table 1), focusing

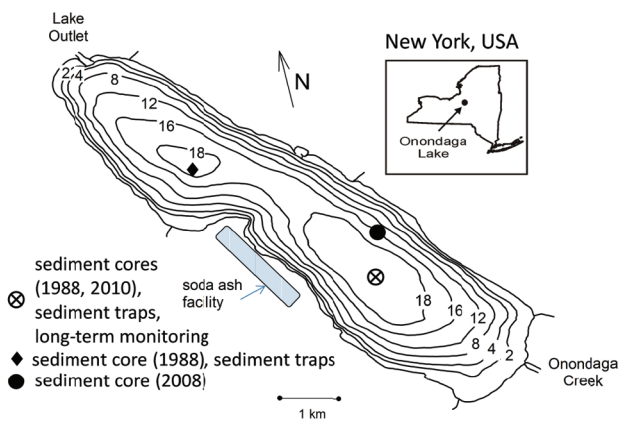

Fig. 1. Onondaga Lake bathymetry, setting, locations for cores, traps and water-column monitoring.

 DOI: 10.5268/IW-2.1.454

Table 1. Timing of perturbations and horizon depths in pelagic sediments for Onondaga Lake.

Horizon No.	Horizon Year	Perturbation	Horizon Depth[+] (cm)	Signature Basis	Core Year	Source
1	1987 (1[x])	closure of soda-ash facility, plus 1 year	13	vertical shift from 1988 to 2008; decrease in particulate inorganic C	2008[†]	
2	1976 (2[x])	treatment at steel factory reduces metals input	22	Cr, Cd, Ni, Zn and Pb	1988	Rowell 1996
3	1971 (2)	P detergent ban	29 30	P	2008[†] 2010	Unpubl. data
4	1970 (2)	Hg loading decrease (95%)	29.5	Hg	1988 2008[†]	Rowell 1996
5	1963 (1)	bomb testing, peak	34 35	C_s-137 C_s-137	1988 2008[†]	Rowell 1996
6	1953 (2)	bomb testing, start	43	C_s-137	2008[†]	
7	1946 (2)	Hg industrial discharge commenced	43 47	Hg	1988 2008[†]	Rowell 1996
8	1939–1943 (2)	Cr steel commences, World War II	46 55	Cr	1988 2008[†]	Rowell 1996
9	1900–1910 (2)	steel production commences	63–73	Cu, Zn, Pb	1988	Rowell 1996
10	1884 (1)	soda-ash production commences	73	diatom community composition	1988	Rowell 1996

[+] for 2008
[x] 1 – primary horizon, 2 – secondary horizon
[†] unpublished data, Bopp RF (2011), pers. comm., Rensselaer Polytechnic Institute.

on those features that contribute to an analysis of the lake's sedimentation regime by imparting horizon(s) in the paleolimnological record (see Effler 1996, for more complete review of history). The horizon information is based on analyses of 3 sediment cores from the south basin of the lake (Fig. 1) collected in 1988 (Rowell 1996), 2008 (unpubl. data), and 2010 (Upstate Freshwater Institute 2011). Fine vertical-scale laminations in the profundal sediments indicate no (or very limited) mixing of the surficial sediments, and thus the historic integrity of the paleolimnological record is retained (Rowell and Effler 1996). A soda-ash (Na_2CO_3) manufacturing facility operated along the shores of Onondaga Lake for the period 1884–1986 and utilized the lake for the disposal of ionic calcium, sodium, and chlorine (Ca^{2+}, Na^+, and Cl^-, respectively; Effler and Matthews 2003) and mercury (Hg; Todorova et al. 2009) wastes. The magnitude of the ionic waste discharge was stoichiometrically coupled to Na_2CO_3 production (Effler and Matthews 2003). This production increased in an approximately linear manner until about 1940, followed by a more uniform level until the facility closed in the late 1980s (Fig. 2a). As a consequence of Hg inputs from this source, the sediments (e.g., Fig. 2b), water column, and biota of the lake are contaminated with Hg (Todorova et al. 2009). A remediation program is underway to abate the residual impacts of the industry's Hg discharge, which includes mobilization of methyl-Hg from profundal sediments in late summer (Todorova et al. 2009). The plan for this program employs an array of technologies (e.g., dredging and capping), but it also relies on the benefits of continuing burial of profundal sediments (Fig. 2b; Hurteau et al. 2010). This reliance on sediment burial is referred to as monitored natural recovery (MNR).

Allochthonous sediment inputs are primarily in the form of clay minerals (Effler et al. 2002). A disproportionately large fraction (~60%) of the total contemporary load of this material enters from a single tributary, Onondaga Creek (Fig. 1), associated with inputs from hydrogeologic

structures described as "mudboils" (Prestigiacomo et al. 2007), first documented in 1899 (Kappel et al. 1996). However, entry of clay mineral loads into pelagic portions of the lake was apparently more limited during operation of the soda-ash industry (Hurteau et al. 2010) because the high in-lake Ca^{2+} concentrations destabilized these particles causing aggregation (Weilenmann et al. 1989) and nearshore deposition (Auer et al. 1996).

Onondaga Lake was continuously oversaturated with respect to calcite throughout the water column before closure of the soda-ash facility. At that time, Ca^{2+} concentrations averaged ~450 mg L^{-1}, and the greatest degree of oversaturation was within the productive epilimnion (Effler and Driscoll 1985). These unusual conditions, promoted by the high Ca^{2+} levels sustained by the industry's ionic waste input, caused extensive $CaCO_3$ precipitation and deposition (Yin and Johnson 1984), and prevented dissolution of depositing $CaCO_3$ (Effler and Driscoll 1985). Despite the ~65% decrease in Ca^{2+} concentration in the lake that resulted from closure of the industry, in-lake equilibrium conditions (i.e., oversaturation) with respect to calcite did not change substantially (Driscoll et al. 1996). $CaCO_3$ was reported to be the dominant constituent in a lake-wide survey (1987) of the surficial sediments, with higher concentrations than observed for other calcareous lakes (Auer et al. 1996), presumably associated with enhanced precipitation and deposition from the industrial Ca^{2+} loading.

Deposition from sediment traps

Deposition from the lake's epilimnion has been assessed annually in a long-term sediment trap program conducted since 1980 (exceptions 1982–1984; Hurteau et al. 2010), using accepted trap design (aspect ratio = 6, diameter = 7.6 cm) and deployment (below epilimnion [10 m], weekly collections; Fig. 1) protocols (Bloesch and Burns 1980, Bloesch 1996) for the April–October interval. Shorter-term trap studies at multiple longitudinal and vertical deployment positions have established the general representativeness of the long-term collection site (Fig. 1) for the lake's pelagic waters and eliminated resuspension (e.g., sediment focusing) as a significant process during summer stratification (Effler and Brooks 1998). Coverage of the winter period (including under the ice) has been much more limited. Winter results are presented here for a single long-term (Nov 2010–Mar 2011) deployment as part of the analysis of consistency of trap fluxes and SAR.

$CaCO_3$ was the dominant component of downward flux of suspended particulate material (DF_{SPM}) over the entire collection program (Hurteau et al. 2010). The DF_{SPM} decreased 51% following the closure of the soda-ash facility (Fig. 2c), driven largely by the 57% decrease in $CaCO_3$ deposition, which was similar to the decrease in Ca^{2+} (Hurteau et al. 2010). The contribution of $CaCO_3$ to DF_{SPM} before closure of the soda-ash facility averaged 81% and decreased to 66% following closure (Hurteau

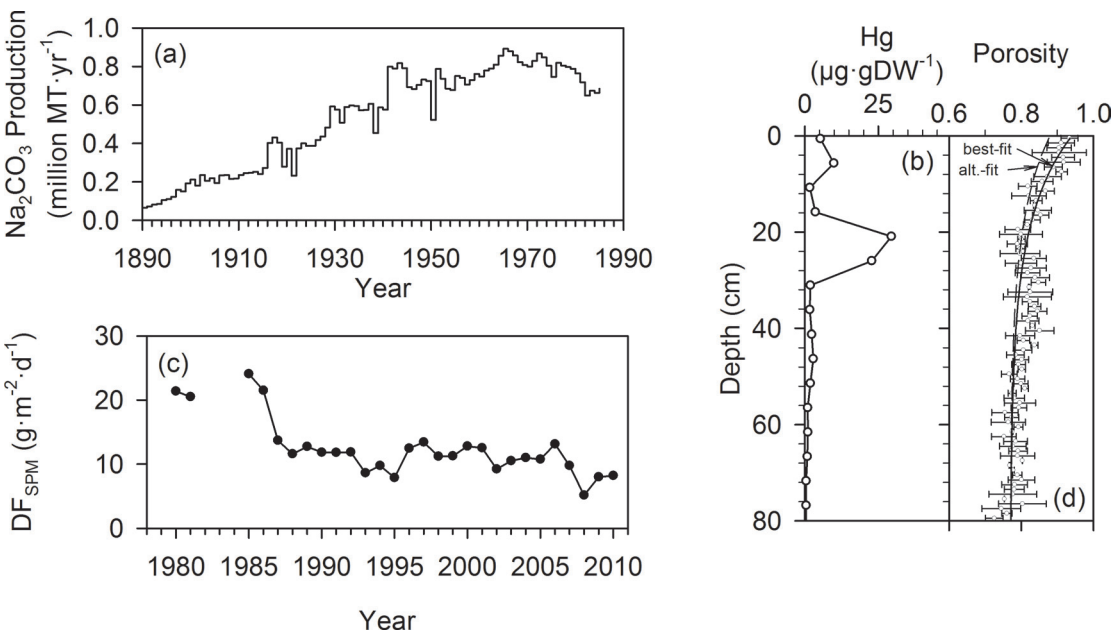

Fig. 2. Information supporting model development and testing: (a) production record for soda-ash (Na_2CO_3), from Effler and Matthews (2003); (b) sediment profile for Hg for core collected in 1988, from Rowell (1996); (c) time series of DF_{SPM} annually for the 1980–2009 period for the mid-May to mid-Sep interval from weekly collections, from Hurteau et al. (2010); and (d) porosity (ϕ) profile with variability bars as ±1 standard deviation, from Gawde (2011).

 DOI: 10.5268/IW-2.1.454

et al. 2010). The average contribution of organic material to deposition has remained largely unchanged (18.5% before, 16.5% after; Hurteau et al. 2010). The contribution of allochthonous (i.e., mostly clay minerals) particulates to deposition increased substantially from <2% before closure of the industry to ~17% following closure, consistent with less near-shore deposition in response to reductions in Ca^{2+} (Hurteau et al. 2010). There has been a shift to even greater contributions by allochthonous inputs within the post-closure interval (e.g., representing ~30% of deposition over 2006–2010; Hurteau et al. 2010).

Modeling

Mass balance model for SAR. The accumulation of solids in the sediments was modeled using a coordinate system whose origin is located at the moving sediment–water interface, wherein sediment layers are buried (advected) downward, as described by Chapra and Reckhow (1983). The rate of burial is influenced by compaction, and potentially by diagenetic losses of the organic fraction; however, the effect of diagenetic losses in this system, and most others (Berner 1980), is inconsequential. The vertical distribution of sediment porosity is described by the following exponential model (Chapra and Reckhow 1983):

$$\phi(z) = \phi(\infty) + [\phi(0) - \phi(\infty)]e^{-\beta z}, \quad (1)$$

where $\phi(z)$, $\phi(\infty)$, and $\phi(0)$ are the porosities at depths z, below the zone of compaction, and zero (i.e., sediment–water interface), respectively, and β is an empirically derived parameter (m^{-1}) specifying the downcore trajectory of compaction. Compaction is complete [$\phi(z) \approx \phi(\infty)$], for $z > \sim 3/\beta$. The burial rate is related to porosity by

$$v_{b,z}\rho_s[1 - \phi(z)] = v_{b,\infty}\rho_s[1 - \phi(\infty)], \quad (2)$$

where $v_{b,z}$, and $v_{b,\infty}$ are the burial velocities at depths z and below the zone of compaction, respectively (m yr^{-1}), and ρ_s is the density of particulate matter (g m^{-3}).

At the sediment–water interface, the SAR (SAR; g m^{-2} yr^{-1}) balances the burial velocity, described by

$$SAR = v_{b,0}[1 - \phi(0)]\rho_s, \quad (3)$$

where $v_{b,0}$ is the burial velocity (m d^{-1}) at the sediment–water interface. Extending equation 2 to the sediment–water interface yields

$$v_{b,0} = \frac{v_{b,\infty}[1 - \phi(\infty)]}{[1 - \phi(0)]}, \quad (4)$$

Now equation 3 and 4 can be combined and solved for the burial velocity at depth below the zone of compaction:

$$v_{b,\infty} = \frac{SAR}{[1 - \phi(\infty)]\rho_s}, \quad (5)$$

The burial velocity of solids at any particular depth can then be calculated as a function of SAR by substituting equation 1 and 5 into equation 2, as described by

$$v_{b,z} = \frac{1}{1 - \phi(\infty) - [\phi(0) - \phi(\infty)]e^{-\beta z}}\left(\frac{SAR}{\rho_s}\right), \quad (6)$$

Alternately, for the case of independent estimates of $v_{b,z}$ being available from dated sediment horizons as described for Onondaga Lake (Table 1), the equation can be solved to determine the historic values of SAR, given the availability of data to specify ρ_s, $\phi(0)$, $\phi(\infty)$, and β. Values for ρ_s, $\phi(0)$, $\phi(\infty)$, and β, determined independently for the Onondaga Lake sediments, are 2.5 g cm^{-3} (Gawde 2011) and 0.88, 0.77, and 6 m^{-1}, respectively (see Fig. 2d for $\phi(z)$ values).

The horizon depth, z_H, defined as the burial depth occurring from some earlier time t to the present time t_p, is given by

$$z_H = \int_t^{t_p} v_{b,z}\, dt, \quad (7)$$

Observations of z_H for various historical events described above are used to test this model for the 1880−2008 period.

System-specific conceptual model for driving SAR. A simple conceptual model was adopted in this study for SAR during the manufacture of soda-ash, which tests the hypothesis that the increase in SAR above the baseline (i.e., what prevailed before production) was associated with production of this chemical. Embedded within this conceptual model are multiple linkages and associated assumptions (Fig. 3) that are well supported by the available information, as well as the value of the baseline SAR. The baseline SAR obtained from equation (5) is 0.5 kg m^{-2} yr^{-1}, based on a burial velocity (v_b) of 0.09 cm yr^{-1}, which is within the range (0.07–0.12 cm yr^{-1}) reported from carbon-14 dating of deeper sediments from a core collected from the south basin in 1988 (Rowell and Effler 1996). The linear couplings between soda-ash production and Ca^{2+} waste load to the lake and in-lake Ca^{2+} concentrations (Fig. 3) are well established (Effler 1996, Effler and Matthews 2003).

The final implicit assumption in the conceptual model is that deposition of $CaCO_3$, and thereby SAR, was regulated by the in-lake Ca^{2+} concentration during

the production of the soda-ash (Fig. 3). This simplistic approach is supported by the dominance of $CaCO_3$ in the depositing sediment (Hurteau et al. 2010) and lake cores (Rowell 1996) and the similarities of both the abrupt decreases of in-lake Ca^{2+} and DF_{SPM} reported following closure of the industry (Womble et al. 1996, Hurteau et al. 2010)

The overall annual SAR (g m^{-2} yr^{-1}) was simulated according to the following empirical expression:

$$SAR = SAR_b + a\, P_{SA}, \quad (8)$$

where SAR_b is the annual background SAR (g m^{-2} yr^{-1}), P_{SA} is the annual soda-ash production (MT yr^{-1}; Fig. 2a), and a is an empirical coefficient (g m^{-2} MT^{-1}). Application of this relationship tests the hypothesis that the increases in SAR during soda-ash manufacturing were linearly related to the chemical production by the industry.

Model calibration, sensitivity, and applications. The sediment model was calibrated through adjustments in the coefficient a (equation 8) to match the 3 primary age horizons in the sediment record identified in core samples (Table 1). The 3 primary horizons targeted in the calibration were the commencement of soda-ash production (1884), the Cs-137 peak (1963), and the closure of the soda-ash facility (1986, plus 1 year for flushing), that, for a 2008 sediment-water interface, were resolved at depths of 73, 34, and 13 cm, respectively (Table 1). The other (n = 7) available horizons (Table 1) serve as an additional test of model performance. Simulations commenced with the 1880 sediment horizon. Adjustments in a were iterated to match the horizons, and associated layers of sediment were accumulated at a 1 year time step.

Sensitivity analyses were conducted for the period of soda-ash production at limits ±10 and 20% of the calibration timeseries of SAR. The calibrated model was used as an analytical tool to quantify (1) the increase in deposition caused by the soda-ash production, (2) the effect of compaction on burial velocity, (3) the effects of the history of SAR dynamics on the vertical features of the paleolimnological record, and (4) the kinetics of diagenesis of sedimentary particulate organic nitrogen.

Results and discussion

Model calibration: performance and SAR and burial velocity timeseries

A value of 0.00535 g m^{-2} MT^{-1} for the coefficient a (equation 8) performed well in simulating the observed primary and secondary horizons from the paleolimnological record (Fig. 4a). The robust array of horizons, mostly driven by the disturbances and perturbations from local waste discharges (Table 1), provided a rigorous test of the model's performance. The use of Pb-210 dating alone could not match this rigor for this particular system. The dates for the horizons were particularly definitive extending back to the mid-1940s (Table 1), supporting a high degree of confidence in general features of the SAR (Fig. 4b) and v_b (Fig. 4c) time series over the 1946–1987 period.

The good performance of the SAR model over the period of soda-ash manufacturing is supportive of the conceptual model that links the production of this chemical to the downward flux of sediment (Fig. 3). Specifically, the success of the SAR model supports the hypotheses that (1) the waste inputs (Ca^{2+}) from this industry were primarily responsible for the increases in SAR, and (2) the increases were linearly related to the soda-ash production of that facility. Moreover, the documented performance of the model supports the parsimony of the adopted modeling approach. Other factors, such as temperature (Strong and Eadie 1978), primary production and its effect on pH (Effler et al. 1981, Koschel et al. 1983, Hodell et al. 1998, Homa and Chapra 2011), and the availability of nucleation sites (Dittrich and Obst 2004), have been reported to influence the rate of $CaCO_3$ precipitation in Ca^{2+}-rich lakes. However, it was not necessary to represent these interactions, and the attendant increased complexity, to achieve good model performance (Fig. 4a). None of these alternate factors

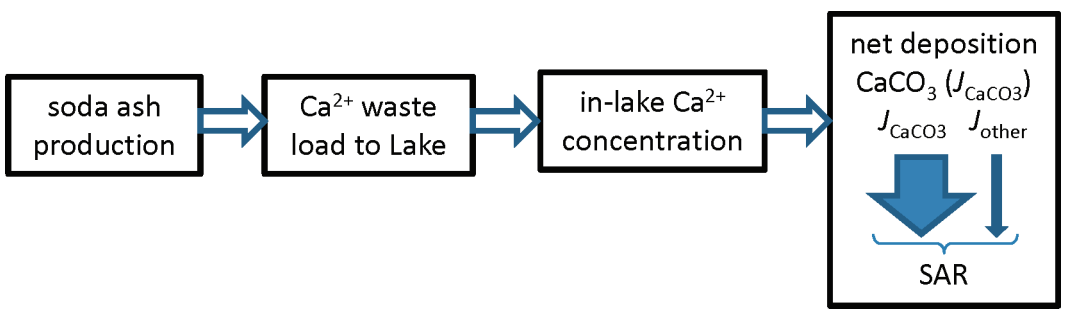

Fig. 3. Conceptual model coupling soda-ash production to SAR, with embedded linkages.

 DOI: 10.5268/IW-2.1.454

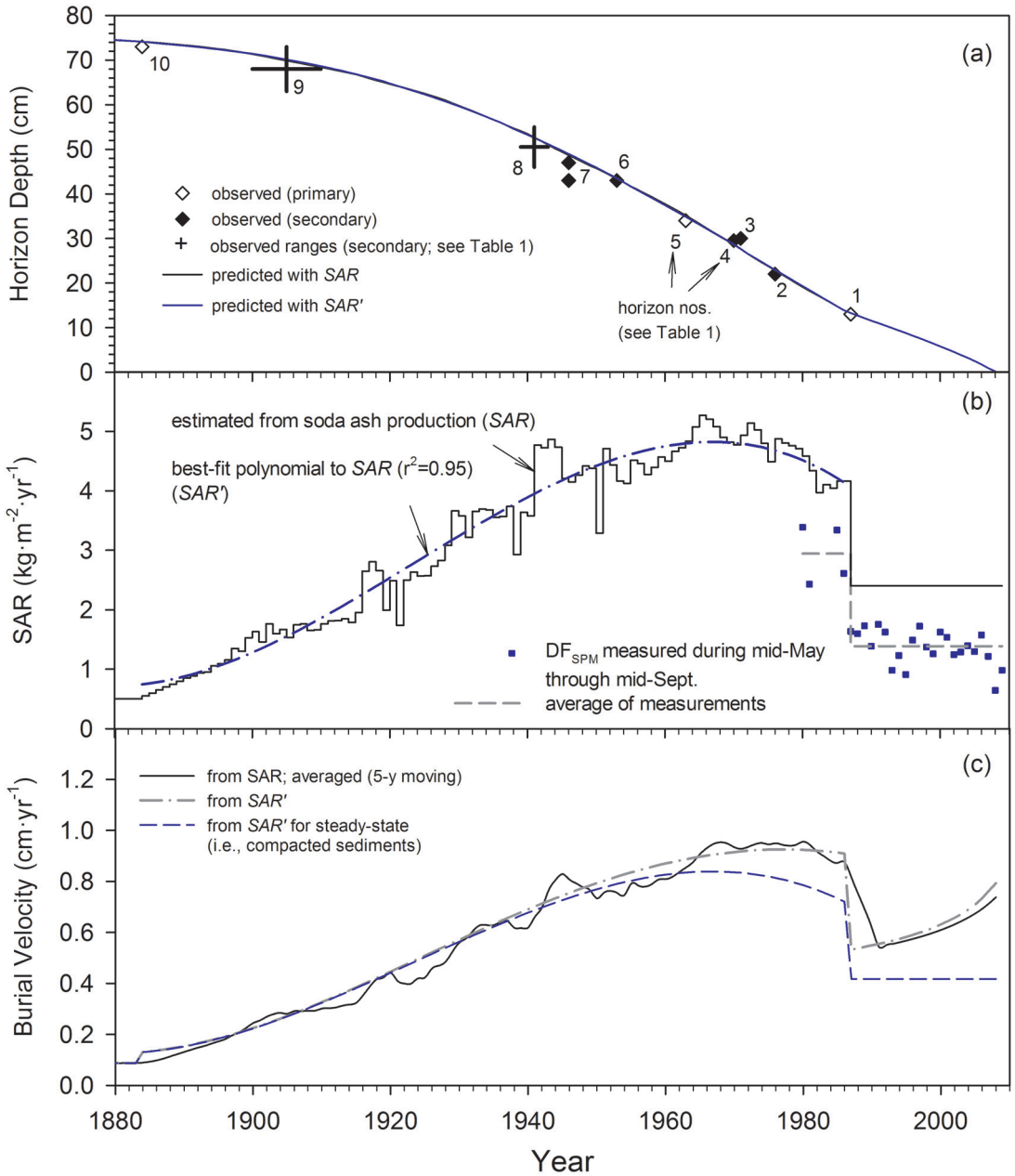

Fig. 4. Modeling: (a) calibration performance for primary sediment date horizons and with respect to secondary horizons (Table 1); (b) calibrated specification of time series of SAR for modeled period, with annual time-step specified according to soda-ash production and alternatively by best-fit polynomial for the production period, and with time series of DF_{SPM} (downward flux of suspended particulate material) for the mid-May to mid-Sep interval, (4 months total) 1980–2009; and (c) calibrated model calculations of burial velocity (v_b): (i) from SAR, as 5-year moving average, (ii) from SAR', and (iii) from SAR' for compacted sediments in upper layers.

offer the possibility of similar success in supporting calibration based on their known histories for this system (Effler 1996).

The timeseries of SAR that emerged from calibration of the model (Fig. 4b) tracked the dynamics reported for the soda-ash production record (Fig. 2a). The maxima during the period of soda-ash manufacturing in the late 1960s (>5 kg m^{-2} yr^{-1}) were more than 10-fold greater than specified for the interval before this chemical production commenced. The year-to-year differences in SAR represented in this calibration reflect the structure of the conceptual model (equation 8) and its dependence on annual soda-ash production but could not reasonably be resolved from this paleolimnological record. For example,

a polynomial fit to this timeseries of SAR (SAR'; Fig.4b) supported equivalent predictions of the sediment horizons (Fig. 4a). The SAR determined for the interval after closure of the industry (~2.4 kg m^{-2} yr^{-1}) was >2-fold lower than the maxima during production, but was nearly 5-fold greater than the pre-industry estimate (Fig. 4b). The predicted decrease in SAR following closure (42%) was generally consistent with the observed decrease (53%) in summertime (mid-May to mid-Sep) downward fluxes reported from sediment trap deployments (Hurteau et al. 2010; Fig. 2c). Temporal uniformity was assumed for the most recent (post-closure) interval, which is roughly consistent with the pattern of summertime sediment trap observations (Fig. 4b). The historic changes in SAR are manifested in the character of the trajectory of the sediment depth versus age relationship (Fig. 4a), with shifts to increased vertical separation of time intervals during periods of increased soda-ash production and a decrease following closure, albeit modest because of limited compaction of recent (upper) sediments.

Two representations of the predicted time series of burial velocity (v_b) that also emerged from the calibration of the SAR model are presented (Fig. 4c), including (1) a 5-year moving average developed from the annual time step SAR values, and (2) based on the polynomial fit of the SAR time series. The vertical details of v_b in the 5-year moving average representation are also likely beyond the practical limits of resolution with common dating protocols. In contrast, the temporal resolution embedded within the polynomial fit was well resolved by the array of sediment horizons (Fig. 4a). The value of v_b increased from <0.1 cm yr^{-1} before operation of the industry (e.g., 1880) to nearly 1 cm yr^{-1} before the facility's closure in the late 1970s, and abruptly decreased following closure (<0.6 cm yr^{-1}; Fig. 4c). The deviations in the v_b temporal pattern from that presented for SAR (Fig. 4b) reflect the effects of increases in porosity (incomplete compaction) of the more recent sediments with the approach to the sediment–water interface (Fig. 2d). This effect is most dramatic within the uppermost 10 cm (e.g., since closure), manifested as progressive increases in v_b with the approach to the interface (Fig. 4c).

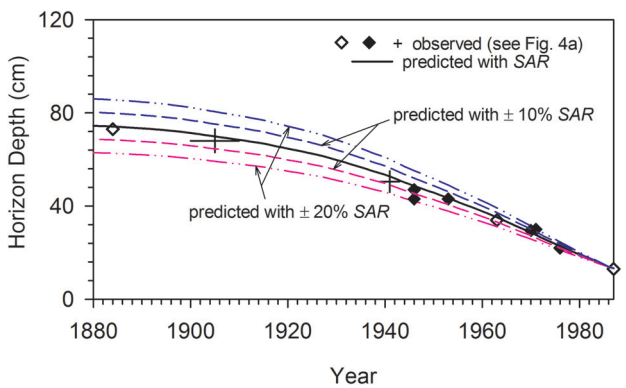

Fig. 5. Sensitivity analyses for horizon dates and depths for the calibrated sediment accumulation model for the period 1880–1987: limits set at ±10% and ±20% of the time series of SAR for the period of soda-ash production.

Model uncertainties

The results of sensitivity analyses on the effects of uncertainty in the calibration time series of SAR indicate a 20% level is overly conservative, bounding the observed sediment horizons by a broad margin (Fig. 5). The 10% level of uncertainty in the history of SAR provides a more reasonable representation of uncertainty during soda-ash production (e.g., most of the horizons continue to be bounded for this case; Fig. 5).

The horizon delineating 1987 (post-closure) is particularly well supported by the consistent downward shifts (13 cm) of multiple horizons from the 1988 core to the 2008 core, as well as a coincident decrease in Ca^{2+} content (Table 1). The uniformity assumption for the interval since the industry closure for the model (SAR), despite the modest decreasing trend in DF_{SPM} (~1.2% per year, $p = 0.014$), is a practical and appropriate simplification. As a practical matter, the indicated recent minor decreases may be difficult to independently resolve from sediment analyses and are exacerbated by the limited extent of compaction of these near-surface sediments. The greatest uncertainty is associated with the adopted baseline SAR of 0.5 kg m^{-2} yr^{-1}. This value is somewhat higher than the 1850 reference values developed in the review of >200 European Lakes (e.g., 0.3 to 0.4 kg m^{-2} yr^{-1} for lowland high alkalinity lakes; Rose et al. 2011). The unusually high background (i.e., natural) Ca^{2+} concentration of this lake, combined with early anthropogenic impacts (Rowell 1996), provides some justification for the somewhat higher background–reference level. Given other system-specific anthropogenic perturbations before the beginning of soda-ash production, such as lowering of the lake by ~0.6 m (1822) and salt production and processing along the lake shore (1800s; Rowell 1996), we cannot eliminate the possibility that the baseline SAR was even greater than 0.5 kg m^{-2} yr^{-1}. Future sediment dating initiatives should target the pre-soda-ash production interval, which could enhance the representation of the relative impact of the soda-ash industry.

Despite the uncertainty in SAR before soda-ash production, it has clearly remained substantially higher after closure of this industry (Fig. 4a), which is qualitatively consistent with the contemporary status of the lake with respect to sediment origins. All 3 of the origin types

 DOI: 10.5268/IW-2.1.454

for particulate matter deposition, primary production, autochthonous precipitation of $CaCO_3$, and allochthonous inputs (Prestigiacomo et al. 2007, Effler and O'Donnell 2010, Hurteau et al. 2010) remain elevated compared to conditions before soda-ash production. Primary production levels are probably the least important, given the modest contribution organic material presently makes to contemporary deposition (Hurteau et al. 2010), although its influence on contemporary $CaCO_3$ precipitation (Koschel et al. 1983) cannot be discounted. Residual inputs from the industrial site (Matthews and Effler 2003) are responsible for ~30% of the contemporary lake Ca^{2+} (Effler and Matthews 2003). The coincident decreasing patterns of in-lake Ca^{2+} concentrations and DF_{SPM} following closure of the industry suggest further decreases in $CaCO_3$ deposition would occur with additional reductions in residual waste inputs. Contemporary allochthonous inputs of clay mineral particles are doubtless substantially greater than before the industry (1896), particularly from the contributions of the mudboils (Prestigiacomo et al. 2007). Moreover, more of this external clay load is reaching the pelagic waters of the lake since the decreases in Ca^{2+} concentrations that followed closure (Hurteau et al. 2010).

Extension of SAR findings from a single core, or from multiple cores from the same site, throughout the deposition zone (Rowan et al. 1992) is accompanied by uncertainty (Rowan et al. 1995), even if systematic gradients in the water column are lacking, such as in Onondaga Lake (Effler 1996). However, there is evidence that the SAR and v_b patterns developed here are generally representative of conditions over the lake's deposition zone. Uniformity within the south basin of the lake is supported by the consistency of horizons observed in 3 different cores (Table 1), 2 collected at a location with near-maximum water depth (~19.5 m; proximate to the long-term sediment trap deployment site), the other where the depth is ~16 m (Fig. 1). Analyses of paired sediment trap (Effler and Brooks 1998) and core (Rowell and Effler 1996) collections from deep-water locations in the south and north basins suggest these fluxes are somewhat higher in the south basin, but only by a modest margin. The average ratio of DF_{SPM} values for 11 paired weekly summertime deployments in 1993 at the long-term site in the south basin and at a deep-water location in the north basin (south ÷ north) was 1.2 (Effler and Brooks 1998). The average flux was 30% higher at the south site ($p < 0.001$, paired t-test) based on 11 two-week deployments in 2009 (unpubl. data). Sediment stratigraphies were reported to be qualitatively similar for a number of constituents in cores collected from the south and north basins in 1988 (Rowell and Effler 1996). Cs-137 peaks occurred at similar depths, with associated sedimentation rate estimates (v_b) for the 1964–1988 interval of 0.88 and 0.83 cm yr^{-1} for the south and north sites (within 6%; Rowell and Effler 1996), indicating greater uniformity during soda-ash production. The larger contemporary differences indicated by trap results are consistent with the increased relative contribution of allochthonous inputs since closure of the soda-ash facility, and the position of the Onondaga Creek input (Fig. 1). The SAR patterns reported here are likely within 10–15% of an integrated average for the deposition zone for the soda-ash production period and within 20–30% for the post-closure period.

Model applications

The effect of anthropogenic drivers on the quantity of sediment accumulated in the lake was represented by comparing the observed trajectory of sediment horizons to the model simulated case of SAR = 0.5 kg m^{-2} yr^{-1} (the background value) maintained throughout the record (Fig. 6). Accordingly, conditions of 1880 would be manifested at a sediment depth of ~16 cm, rather than the observed ~76 cm (Fig. 6). The difference, ~60 cm, is a reasonable representation of the sediment added from anthropogenic effects, primarily from soda-ash production in the form of $CaCO_3$.

The effects of incomplete compaction of the upper portions of the sediment on the burial velocity, v_b, were resolved by comparing the model simulation of the v_b time series for a fully compacted (below the zone of compaction) porosity case, (∞), to that obtained from calibration (Fig. 4c). The patterns converge in ~1950. The fully compacted model scenario depicts what the v_b values of the most recently deposited sediments will be after several decades of the operation of this process. The

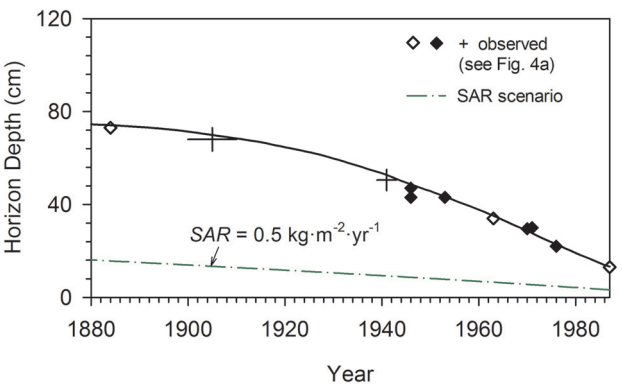

Fig. 6. Model application: comparison of simulation of sediment accumulation for the case of an unchanging SAR that prevailed before the industry throughout the record, to the observed calibrated case.

effects of compaction are substantial in this lake, particularly for the first 20–30 years (or upper 15 cm). For example, the burial velocity of the most recent sediments, ~0.8 cm yr^{-1}, will decrease to ~0.4 cm yr^{-1} when fully compacted (Fig. 4c).

The diluting effects of the elevated SAR levels from soda-ash production are depicted for 2 selected particulate constituents, Hg and phosphorus (P; Fig. 7a and b), by invoking lower (and constant) SAR values in model simulations. Two SAR values were considered (0.5 and 2.4 kg m^{-2} yr^{-1}) corresponding to conditions before the start of production and since closure of the facility (Fig. 4b). The modeling approach was to establish the history of the downward fluxes of the 2 constituents from the calibrated history of SAR and the observed sediment profiles. The scenario changes in SAR (0.5 and 2.4 kg m^{-2} yr^{-1}), together with the established downward fluxes of each constituent, were used to predict the scenario sediment profiles. The prevailing vertical patterns of ϕ (Fig. 2d) and ρ_s (Gawde 2011) and the simplifying assumption of no diagenetic effects were adopted for these simulations. The predicted profiles for these different SAR levels for Hg (Fig. 7a) are for a 1988 sediment–water interface, while those for P (Fig. 7b) are for a 2010 interface. Predictions for all these scenarios depict the major diluting effect the high levels of SAR from soda-ash production had on the concentration profiles (Fig. 7). The absence of the dilution effect leads to increased concentrations over narrower sediment depth intervals and shifts in these historic peaks upward toward the sediment–water interface. The effect is greater for the lowest SAR.

The model was additionally applied to investigate the kinetics of diagenesis of an important component of particulate organic matter, particulate organic nitrogen (PON), based on changes in the PON profiles of core samples collected at the same location (Fig. 1) in 1995 (Fig. 8a) and 2010 (Fig. 8b). Years were assigned to depth intervals of the cores from the time series of SAR determined from calibration (Fig. 4b), which allows the specification of the corresponding PON concentrations for these layers in the cores (Fig. 8a and b). First-order decay rates (k) for the 15 years between the core collections were calculated (Fig. 8c). Most of the annual decay rates determined in this manner were between 0.01 and 0.07 yr^{-1}. Sediments in the age range of 15–40 years demonstrated decreases in k as the age of sediment increased (Fig. 8d). The strong logarithmic relationship for this age range, depicting the age dependency of sediment diagenesis for PON (Fig. 8d), is consistent with a form reported in the literature (Middelburg 1989).

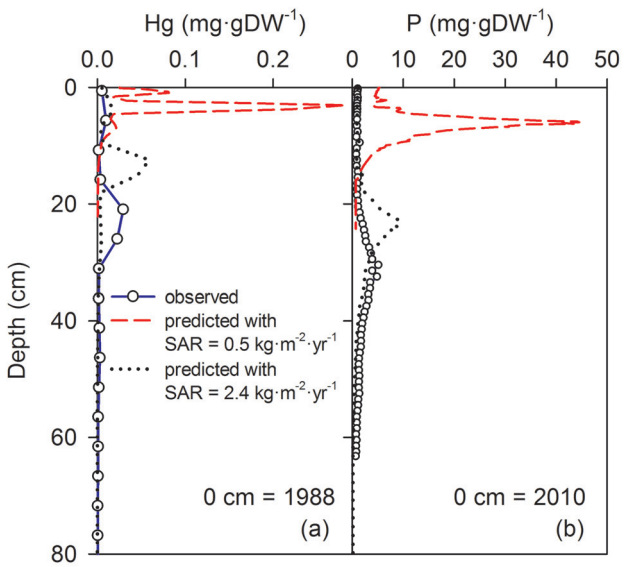

Fig. 7. Model applications depicting the diluting effect of the high SAR(s) from soda-ash production, with 2 hypothetical low SARs that correspond to pre- and postproduction levels: (a) Hg, 1988 profile; and (b) particulate P, 2010 profile.

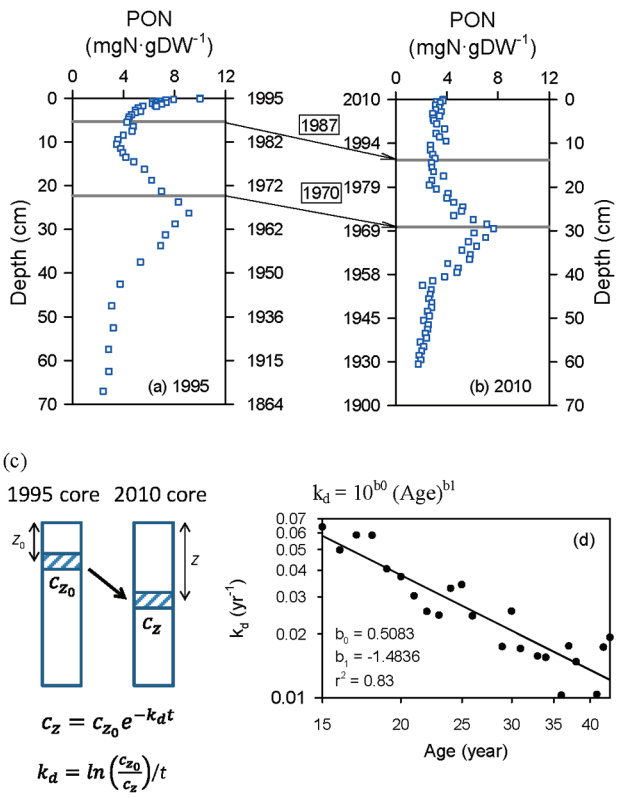

Fig. 8. Model application to evaluate kinetics of diagenesis: (a) sediment profile of PON for core sample collected in 1995, with 1987 and 1970 horizons identified; (b) sediment profile of PON for core sample collected in 2010, with 1987 and 1970 horizons identified; (c) concept schematic for calculation of diagenesis decay rate, k_z; and (d) evaluation of the dependency of k_z on sediment age.

DOI: 10.5268/IW-2.1.454

The SAR model also serves as the physical submodel of a larger sediment diagenesis model being used to project responses to rehabilitation measures targeting decreases in primary production (Gelda et al., unpubl.). While the particular driver for this case study is system-specific, the mass balance constructs of the SAR model (equations 1–7) and the form of the analytical capabilities demonstrated above, are broadly applicable. What must be developed on a system-specific basis is a sound relationship between the driver(s) and SAR (e.g., equation 8), such as the primary production from cultural eutrophication or erosion-based inputs that have caused increased SAR.

Extent of closure between SAR and DF_{SPM}

Given the rich array of sediment horizons (Rowell 1996) and the inherent integration of year-round net deposition embedded in the sediment record, a comparison of the temporal limitations of trap deployments to SAR may be viewed as a reasonable basis to evaluate the consistency of the measurements of DF_{SPM}. Two features of the trap program for Onondaga Lake make this a particularly appropriate system for such a comparison: (1) its long tenure and (2) the demonstrated representativeness of these collections for the pelagic waters of the lake during summer stratification (Effler and Brooks 1998).

It is axiomatic that DF_{SPM} will overestimate SAR (beyond the usually small effects of sediment diagenesis) in systems where extensive sediment resuspension occurs because this augments the primary component of downward flux with a secondary component of redepositing sediment (Pennington 1974, Bloesch 1995, 2004). Moreover, extension of fluxes measured during summer stratification to annual values is problematic. Generally, lower DF_{SPM} is observed during the nonsummer months in north temperate lakes (e.g., 25–35% of summertime fluxes), particularly in systems where autochthonous production of organic particles is an important contributor to this flux (Fallon and Brock 1980, Bloesch and Uehlinger 1986, Kleeberg 2002, Chu et al. 2005). For Lake Constance (Switzerland), Stabel (1986) reported the wintertime downward flux of Ca (e.g., $CaCO_3$), the largest component of DF_{SPM}, was greatly diminished compared to summertime fluxes. Direct measurements of DF_{SPM} during ice cover when turbulence is generally low (Wetzel 2001) are rare (Fallon and Brock 1980). The seasonally elevated turbulence at common trap deployment depths during turnover intervals has been reported to cause contributions from resuspension in collections from certain stratifying lakes (Fallon and Brock 1980, Poister and Armstrong 2003, Moschen et al. 2009). Pennington (1974) pursued closure of DF_{SPM} and SAR in 5 stratifying English lakes and reported "reasonable levels of closure" (e.g., within 39%) for the 3 deeper lakes (Windermere, Ennerdale, and Wastewater; maximum depth ≥42 m), but strong signatures of resuspension (DF_{SPM} >2-fold higher than SAR) for the 2 shallowest (Esthwaite and Blelham Tarn; maximum depth ≤ 16 m).

An estimate of the average annual DF_{SPM} for the 1988–2009 interval was developed in this study and partitioned according to seasonal contributions in the context of annual dynamics in the stratification regime (Table 2). The results of the analysis should be considered a reasonable approximation, which acknowledges uncertainties associated with the uneven seasonal coverage of the trap program. Moreover, year-to-year variations in potential drivers such as hydrologic (i.e., allochthonous sediment) loading (Effler 1996), features of the stratification regime (O'Donnell et al. 2010), and timing of ice-cover (Owens and Effler 1996), are known to occur. Robust representation of DF_{SPM} is available for 7 months annually (Apr–Oct) from the long-term trap program (Table 2). We have the greatest confidence in the fluxes from the summertime (mid-May to mid-Sep) trap collections with respect to consistency with SAR because these deployments were below the epilimnion (Bloesch 1996, Hurteau et al. 2010), and no noteworthy resuspension inputs occurred (Effler and Brooks 1998; Table 2). In contrast, the sediment traps were often not within stratified layers in the mid-September through October and April to mid-May intervals because of turnover conditions or deep epilimnetic boundaries (e.g., approach to turnover). Direct measurements of DF_{SPM} in the other 5 months of the year (late fall and winter) have been much more limited, with single observations (1 week deployment) during ice-cover in February 1994 (Penn 1994), and the long-term deployment result for the November 2010–March 2011 interval presented here. The duration of this last long-term deployment is not considered particularly problematic in light of the small contribution of organic sediment to DF_{SPM} (Hurteau et al. 2010), the low temperatures (mostly <5 °C), and the over-saturated conditions with respect to calcite (Driscoll et al. 1994).

The under-the-ice DF_{SPM} was decidedly lower (~5-fold) than the summertime average (Table 2); however, the flux for the other cold months without ice-cover was only ~30% lower. The estimate of the average annual DF_{SPM} for the 1988–2009 interval is 3.12 kg m^{-2} yr^{-1} (Table 2). It exceeds the contemporary SAR by 30%, perhaps reflecting a modest level of resuspension inputs during turnover periods. In the context of uncertainties in the SAR determined through model calibration and the limitations in trap measurements in certain portions of the year, this DF_{SPM} represents

Table 2. An average annual estimate of DF_{SPM} for Onondaga Lake for the 1988–2009 interval, partitioned according to seasonal contributions.

Interval	Months	Observations	Mass/Area Deposited (kg m^{-2})	Avg. DF_{SPM} (g m^{-2} $^{-1}$)	Comments
mid-May to mid-September	4	381	1.39	11.4	traps deployed below epilimnion, well stratified
mid-September through October	1.5	134	0.36	8.1	traps within deepening epilimnion and onset of fall turnover
November to mid-January*	2.5	1	0.67	8.8	turnover, from November–March deployment of 2010–2011
mid-January to mid-March	2	1	0.14	2.3	under the ice, based on 1994 observation (Penn 1994)
mid-March	0.5	1	0.13	8.8	turnover, from November–March deployment of 2010/2011
April to mid-May*	1.5	76	0.43	9.6	traps during spring turnover through the onset of summer stratification
		annual DF_{SPM} = 3.12 kg m^{-2} yr^{-1}			

* estimated by adjusting the flux measured for the November (2010) through March (2011) deployment by the under-the-ice flux of Penn (1994) for 2 months of ice cover.

reasonably good closure with the contemporary SAR (e.g., Pennington 1974). Accordingly, this provides independent support for the most recent portion of the SAR time series determined from calibration (Fig. 4b) as well as supporting the general utility of sediment traps for staying apprised of potential short-term changes in contemporary SAR in this lake that may be difficult to resolve from the sedimentary record.

SAR in Onondaga Lake, in context

The Onondaga Lake SAR (Rose et al. 2011) and DF_{SPM} (Tartari and Biasci 1997, Effler and Brooks 1998, Bloesch 2004) levels before the discontinuation of soda-ash production (Fig. 4a) exceed the upper bounds of ranges included in related reviews for lakes and generally are exceeded only in reservoirs (Ritchie and McHenry 1990). Even the substantially lower contemporary fluxes remain very high relative to other systems, exceeding the DF_{SPM} values for all but 2 of the 40 lakes reviewed by Tartari and Biasci (1997), and all but 1 of the 31 lakes reviewed by Effler and Brooks (1998). The contemporary SAR for the lake exceeds all values included in a compilation of 207 European lakes, derived from Pb-210 dated cores (Rose et al. 2011), supporting Onondaga Lake as an end-member case. The increasing trend reported since 1850 in most (~70%) of the European lakes could be attributed to changes in land-use, agricultural practices, and eutrophication (Rose et al. 2011). In sharp contrast, the major increase in SAR in Onondaga Lake was driven by industrial pollution, mediated primarily by autochthonous production of $CaCO_3$ (Yin and Johnson 1984, Driscoll et al. 1994). This did not change the bulk chemistry of the sediments substantially because of the natural marl composition before the industry (Rowell and Effler 1996).

The estimated mass of these industrial deposits (60 cm thick) is approximately 2.1×10^9 kg (or 2.1 million MT), calculated as the product of $a \cdot P_{SA}$ (equation 8) developed in model calibration and the area of the deposition zone (6.98×10^6 m^2) and summed over 1884–1986 interval. The corresponding loss of lake volume associated with these industrial deposits is ~3%. However, this anthropogenic flux has had an unintended benefit of increased burial and dilution of contaminants, including Hg (Fig. 7a) discharged from the same facility, as well as an array of heavy metals received primarily from a local steel manufacturer (Rowell and Effler 1996). The continued burial of these contaminants, in particular Hg, is a prominent feature (MNR) of a rehabilitation program (NYSDEC 2005) that targets the residual impacts of the industry.

Acknowledgements

This is contribution number 293 of the Upstate Freshwater Institute.

 DOI: 10.5268/IW-2.1.454

References

Auer MT, Johnson NA, Penn MR, Effler SW. 1996. Pollutant sources, depositional environment, and the surficial sediment of Onondaga Lake, New York. J Environ Qual. 25:46–55.

Berner RA. 1980. Early Diagenesis. Princeton, (NJ): Princeton Press.

Bloesch J. 1995. Mechanisms, measurement and importance of sediment resuspension in lakes. Mar Freshwater Res. 46:295–304.

Bloesch J. 1996. Towards a new generation of sediment traps and a better measurement/understanding of settling particulate flux in lakes and oceans: A hydrodynamic protocol. Aquat Sci. 58:283–296.

Bloesch J. 2004. Sedimentation and lake sediment formation. In: O'Sullivan PE, Reynolds CS, editors. The Lakes Handbook, Volume 1. Blackwell Science. p 197–229.

Bloesch J, Burns NM. 1980. A critical review of sediment trap technique. Schweiz Z Hydrol. 42:15–55.

Bloesch J, Uehlinger U. 1986. Horizontal sedimentation differences in a eutrophic Swiss Lake. Limnol Oceanogr. 31:1094–1109.

Blomqvist S, Hakanson L. 1981. A review of sediment traps in aquatic environments. Arch Hydrobiol. 91:101–132.

Chapra SC. 1997. Surface water-quality modeling. New York: McGraw-Hill. 844 p.

Chapra SC, Reckhow KH. 1983. Engineering approaches for lake management, Volume 2: Mechanistic modeling. Boston (MA): Butterworth Publishers.

Chu G, Liu J, Schettler G, Li J, Sun Q, Gu Z, Lu H, Liu Q, Liu T. 2005. Sediment fluxes and varve formation in Sihailongwan, a maar lake from northeastern China. J Paleolimnol. 34:311–324.

Dittrich M, Obst M. 2004. Are picoplankton responsible for calcite precipitation in lakes? Ambio. 33:559–564.

Dittrich M, Wehrli B, Reichert P. 2009. Lake sediments during the transient eutrophication period: Reactive-transport model and identifiability study. Ecol Model. 220:2751–2769.

Doerr SM, Effler SW, Whitehead KA, Auer MT, Perkins MG, Heidtke TM. 1994. Chloride model for polluted Onondaga Lake. Water Res. 28:849–861.

Driscoll CT, Effler SW, Doerr SM. 1994. Changes in inorganic carbon chemistry and deposition of Onondaga Lake, New York. Environ Sci Technol. 28:1211–1218.

Driscoll CT, Effler SW, Doerr SM. 1996. Inorganic Carbon, Ca^{2+}, $CaCO_3$(s), and pH (in, Chemistry, Chapter 5), In: Effler SW, editor. Limnological and engineering analysis of a polluted urban Lake. Prelude to environmental management of Onondaga Lake, New York. New York (NY): Springer-Verlag.

Effler SW. 1996. Limnological and engineering analysis of a polluted urban lake. Prelude to environmental management of Onondaga Lake, New York. New York (NY): Springer-Verlag.

Effler SW, Brooks CM. 1998. Dry weight deposition in polluted Onondaga Lake, New York, U.S.A. Water Air Soil Pollut. 103:389–404.

Effler SW, Driscoll CT. 1985. Calcium chemistry and deposition in ionically enriched Onondaga Lake, New York. Environ Sci Technol. 19:716–720.

Effler SW, Field SD, Meyer MA, Sze P. 1981. Response of Onondaga Lake to Restoration Efforts. J Env Eng Div-ASCE. 107:191–210.

Effler SW, Matthews DA. 2003. Impacts of a soda ash facility on Onondaga Lake and the Seneca River, NY. Lake Reserv Manage. 19:285–306.

Effler SW, O'Donnell SM. 2010. A long-term record of epilimnetic phosphorus patterns in recovering Onondaga Lake, New York. Fund Appl Limnol. 177(1):1–18.

Effler SW, O'Donnell SM, Matthews DA, Matthews CM, O'Donnell DM, Auer MT, Owens EM. 2002. Limnological and loading information and a phosphorus total maximum daily load analysis for Onondaga Lake. Lake Reserv Manage. 18:87–108.

Fallon RD, Brock TD. 1980. Planktonic blue-green algae: Production, sedimentation, and decomposition in Lake Mendota, Wisconsin. Limnol Oceanogr. 25:72–88.

Gawde RK. 2011. Modeling particulate organic matter diagenesis with sed2k [master's thesis]. [Houghton (MI):] Michigan Technological University, Department of Civil and Environmental Engineering.

Hodell DA, Schelske CL, Fahenestiel GL, Robbins LL. 1998. Biologically induced calcite and its isotopic composition in Lake Ontario. Limnol Oceanogr. 43:187–199.

Homa ES, Chapra SC. 2011. Modeling the impacts of calcite precipitation on the epilimnion of an ultraoligotrophic, hard-water lake. Ecol Model. 222:76–90.

Hurteau C, Matthews DA, Effler SW. 2010. A retrospective analysis of solids deposition in Onondaga Lake, New York: Composition, temporal patterns, and drivers. Lake Reserv Manage. 26:43–53.

Kappel WM, Sherwood DA, Johnston WH. 1996. Hydrogeology of the Tully Valley and characterization of mudboil activity, Onondaga County, New York. Water Resources Investigations Report; 96–4043, p 71. Ithaca (NY): US Geological Survey; Branch of Information Services distributor: viii.

Kleeberg A. 2002. Phosphorus sedimentation in seasonal anoxic Lake Scharmützel, NE Germany. Hydrobiologia. 472:53–65.

Koschel R, Benndorf J, Proft J, Recknagel F. 1983. Calcite precipitation as a natural control mechanism of eutrophication. Arch Hydrobiol. 98:380–408.

Matisoff G, Holdren GR. 1993. Historical loading record of sulfur in an Adirondack Lake. J Paleolimnol. 9:243–256.

Matthews DA, Effler SW. 2003. Decrease in pollutant loading from residual soda ash production waste. Water Air Soil Pollut. 146:55–73.

Middelburg JJ. 1989. A simple rate model for organic matter decomposition in marine sediments. Geochim Cosmochim Acta. 53:1577–1581.

Moschen R, Lücke A, Parplies J, Schleser GH. 2009. Controls on the seasonal and interannual dynamics of organic matter stable carbon isotopes in mesotrophic Lake Holzmaar, Germany. Limnol Oceanogr. 54:194–209.

[NYSDEC] New York State Department of Environmental Conservation. 2005. Record of decision: Onondaga Lake bottom subsite of the Onondaga Lake superfund site, Towns of Geddes and Salina, Villages of Solvay and Liverpool, and City of Syracuse, Onondaga County, New York. Albany (NY).

O'Donnell SM, O'Donnell DM, Owens EM, Effler SW, Prestigiacomo AR, Baker DM. 2010. Variations in the stratification regime of Onondaga Lake: Patterns, modeling, and implications. Fund Appl Limnol. 176:11–27.

Owens EM, Effler SW. 1996. Modeling the impacts of a proposed hypolimnetic wastewater discharge on stratification and mixing in Onondaga Lake. Lake Reserv Manage. 12:195–206.

Penn MR. 1994. The deposition, diagenesis and recycle of sedimentary phosphorus in a hypereutrophic lake [dissertation]. [Houghton (MI):] Michigan Technological University.

Pennington W. 1974. Seston and sediment formation in five Lake District lakes. J Ecol. 62:215–251.

Poister D, Armstrong DE. 2003. Seasonal sedimentation trends in a mesotrophic lake: Influence of diatoms and implications for phosphorus dynamics. Biogeochemistry. 65:1–13.

Prestigiacomo AR, Effler SW, O'Donnell DM, Hassett JM, Michelanko EM, Lee Z, Weidemann AD. 2007. Turbidity and suspended solids levels and loads in a sediment enriched stream: implications for impacted lotic and lentic ecosystems. Lake Reserv Manage. 23:231–244.

Rippey B, Anderson N, Renberg I, Korsman T. 2008. The accuracy of methods used to estimate the whole-lake accumulation rate of organic carbon, major cations, phosphorus and heavy metals in sediment. J Paleolimnol. 39:83–99.

Ritchie JC, McHenry JR. 1990. Application of radioactive fallout cesium-137 for measuring soil erosion and sediment accumulation rates and patterns: A review. J Environ Qual. 19:215–233.

Rose N, Morley D, Appleby P, Battarbee R, Alliksaar T, Guilizzoni P, Jeppesen E, Korhola A, Punning JM. 2011. Sediment accumulation rates in European lakes since AD 1850: trends, reference conditions and exceedence. J Paleolimnol. 45:447–468.

Rowan DJ, Cornett RJ, King K, Risto B. 1995. Sediment focusing and ^{210}Pb dating: a new approach. J Paleolimnol. 13:107–118.

Rowan DJ, Kalff J, Rasmussen JB. 1992. Estimating the mud deposition boundary depths in lakes from wave theory. Can J Fish Aquat Sci. 49:2490–2497.

Rowell HC. 1996. Paleolimnology of Onondaga Lake: The history of anthropogenic impacts on lake water quality. Lake Reserv Manage. 12:35–45.

Rowell HC, Effler SW. 1996. Sediment stratigraphy (in Sediments, Chapter 8). In: Effler SW, editor. Limnological and engineering analysis of a polluted urban Lake. Prelude to environmental management of Onondaga Lake, New York. New York (NY): Springer-Verlag. p. 622–666.

Stabel HH. 1986. Calcite precipitation in Lake Constance: Chemical equilibrium, sedimentation, and nucleation by algae. Limnol Oceanogr. 31:1081–1093.

Strong AE, Eadie BJ. 1978. Satellite observations of calcium carbonate precipitations in the Great Lakes. Limnol Oceanogr. 23:877–887.

Tartari G, Biasci G. 1997. Trophic status and lake sedimentation fluxes. Water Air Soil Pollut. 99:523–531.

Todorova SG, Driscoll CT, Matthews DA, Effler SW, Hines ME, Henry EA. 2009. Evidence for regulation of monomethyl mercury by nitrate in a seasonally stratified, eutrophic lake. Environ Sci Technol. 43:6572–6578.

Upstate Freshwater Institute. 2011. Modeling sediment-water fluxes and hypolimnetic redox species patterns with linked sediment (SED2K) and watercolumn (UFILS4) models to inform OLWQM . A technical memorandum prepared for Anchor-QEA. Upstate Freshwater Institute; Michigan Technological University and Tufts University.

[USEPA] United States Environmental Protection Agency. 2005. Contaminated sediment remediation guidance for hazardous waste sites. EPA-540-R-05-012. Office of Solid Waste and Emergency Response. OSWER 9355.0-85.

Weilenmann U, O'Melia CR, Stumm W. 1989. Particle transport in lakes: Models and measurements. Limnol Oceanogr. 34:1–18.

Wetzel RG. 2001. Limnology: lake and reservoir ecosystems. New York: Academic Press.

Womble RN, Driscoll CT, Effler SW. 1996. Calcium carbonate deposition in Ca^{2+} polluted Onondaga Lake, New York, U.S.A. Water Res. 30:2139–2147.

Yin C, Johnson DL. 1984. An Individual particle analysis and budget study of Onondaga Lake sediments. Limnol Oceanogr. 29:1193–1201.

 DOI: 10.5268/IW-2.1.454